Supporting Information

Graphdiyne based separator toward high performance activated electrolyte-enhanced supercapacitors

Na Liang[a], Xueyan Wu[a], Xiuli Zhang[a], Yan Lv[a], Jixi Guo*[a], Renhe Guo[a], Yingfu Zhu[a], Huibiao Liu*[abc], Dianzeng Jia*[a]

[a.]State Key Laboratory of Chemistry and Utilization of Carbon Based Energy Resources; Key Laboratory of Advanced Functional Materials, Autonomous Region
Institute of Applied Chemistry, College of Chemistry, Xinjiang University,
Urumqi, 830046, Xinjiang P.R. China
Email: jxguo1012@163.com; jdz@xju.edu.cn
[b.]CAS Key Laboratory of Organic Solids, Beijing National Laboratory for Molecular Sciences, CAS Research/Education Center for Excellence in Molecular Sciences,
Institute of Chemistry, Chinese Academy of Sciences,
Beijing, 100190, P. R. China
Email: liuhb@iccas.ac.cn
[c.]University of Chinese Academy of Sciences,
Beijing, 100049, P. R. China,

Experimental Section

Materials

Polypropylene membrane (PP, NKK-MPF30AC-100) was purchased from Nippon Kodoshi Corporation. polyvinyl alcohol (PVA 98.0-99.0 mol%) and tetrabutylammonium fluoride (TBAF) were purchased from Aladdin Chemical Reagents, Inc. Unless otherwise stated, other analytical chemicals were used as received.

Synthesis of GDY

Hexaethynylbenzene (HEB) was synthesized according to a reported synthetic method[1]. HEB (20, 25, 30, 35, 40 mg) was dissolved in ethyl acetate and pyridine solution and dropped into copper foil solution containing pyridine. The mixture was heated at 50 °C in nitrogen for 3 days while avoiding light. Then the copper foil coated with GDY membrane was washed several times with acetone. GDY membrane was obtained by drying at room temperature.

Synthesis of GDY/PVA membrane

GDY/PVA membrane was synthesized by in situ composite method. First, PVA (4 g) dissolved in deionized water (50 mL). The blend was heated at 90 °C for 3 h with continuous stirring until the solution became transparent. After that, 8% (w/w) of the PVA solution was prepared. Then the copper foil coated with GDY membranes (20, 25, 30, 35, 40 mg) was placed in a petri dish, 15 mL PVA solution was added, and placed in an oven at 60 °C for 8 h. After drying, the copper sheet was removed and naturally exfoliated. The prepared GDY/PVA composite membranes were denoted as GDY/PVA-20, GDY/PVA-25, GDY/PVA-30, GDY/PVA-35 and GDY/PVA-40, respectively.

Structure characterizations

The FTIR spectra of the samples were recorded by VERTEX70 spectrometer. Scanning electron microscopy (SEM, Japan Hitachi SU-4800) was used to observe the microstructure of the material. TEM image was studied by a JEM 2100F (200 kV) high resolution transmission electron microscopy (TEM). X-ray photoelectron spectroscopy (XPS, VG Scientific ESCALab220i-XL (Al Kα radiation)) was used to determine the surface chemical properties of the material. Structure information of samples was studied by X-ray powder diffraction (XRD, Japan Rigaku D/max-2500 rotation anode X-ray diffractometer and graphite-monochromatized Cu Kα radiation) and Raman spectra (Raman; NT-MDT NTEGRA Spectra). The contact angle was measured with a contact angle meter (JJ2000B2, China Electric Power Corporation). Stress-strain was tested by a microcomputer-controlled electronic universal testing machine (MTS, E44.304) with the tensile speed set at 0.5 mm/min.

Proton conductivity

The ionic conductivity (σ) of the membrane was measured by electrochemical impedance spectroscopy (CHI 770, Shanghai Chenhua Co., Ltd.) in the frequency range of 1 Hz～100 kHz. The 1 cm × 1 cm sample was sandwiched between two stainless steel electrodes at room temperature. The sample was soaked in deionized water before measurement. The transverse σ value of the membrane is calculated from the impedance data using the following formula.

$$\sigma = \frac{d}{R \times S} \qquad (1)$$

where d (cm) and S (cm^2) are the thickness and surface area of the samples, respectively. R originates from the low intersection point between the high frequency semicircle and the Z" axis on the complex

Electrochemical characterization

The electrodes were prepared on stainless steel mesh using activated carbon (AC, 80 wt%), polytetrafluoroethylene (5 wt%), and carbon black (15 wt%). The area loading amount of stainless steel mesh was 5–7 mg cm^{-2}. The capacitance performance of SC was tested on the dual-electrode battery of CHI 760E electrochemical workstation. 1 M H_2SO_4 mixed with HQ aqueous solution as electrolyte. The cell capacitance (C_{Cell}, F g^{-1}), electrode specific capacitance (C_{sp}, F g^{-1}), energy density (E, Wh kg^{-1}) and power density (P, W kg^{-1}) using the following equation[2-7].

$$C_{cell} = \frac{2 \times I \times \Delta t}{M \times \Delta V} \quad \text{.....(2)}$$

$$C_{sp} = 4\, C_{cell} \quad \text{.....(3)}$$

$$E = \frac{C_{cell} \times \Delta V^2}{2 \times 3.6} \quad \text{.....(4)}$$

$$P = \frac{3600 \times E}{\Delta t} \quad \text{.....(5)}$$

Where I is the discharge current (A), Δt is the discharge time (s), ΔV is the potential window (V), and M is the total mass of the active materials used in the two electrodes (mg).

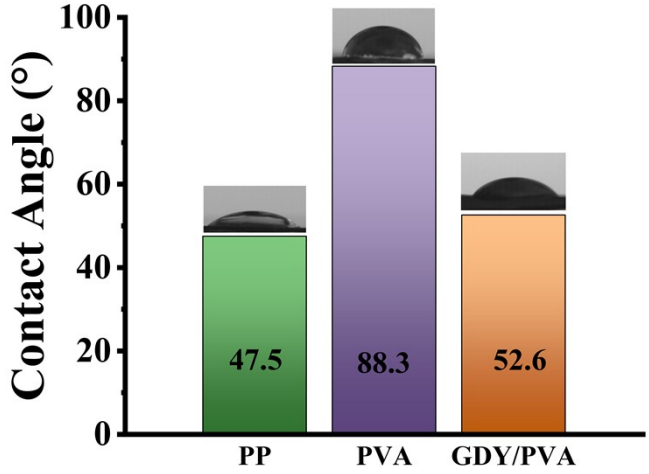

Figure S1. Contact angle of different membranes.

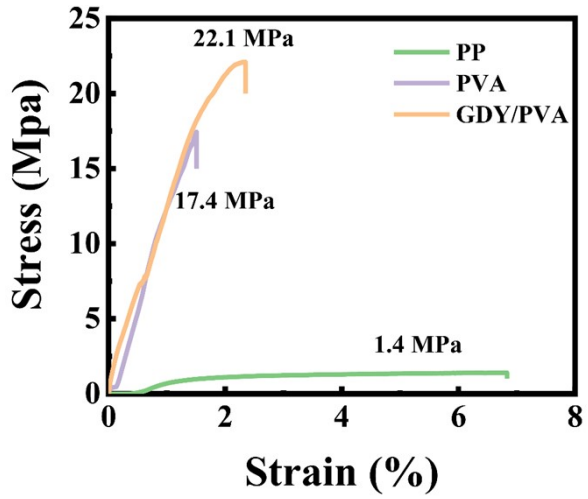

Figure S2. Stress-strain curves of different membranes.

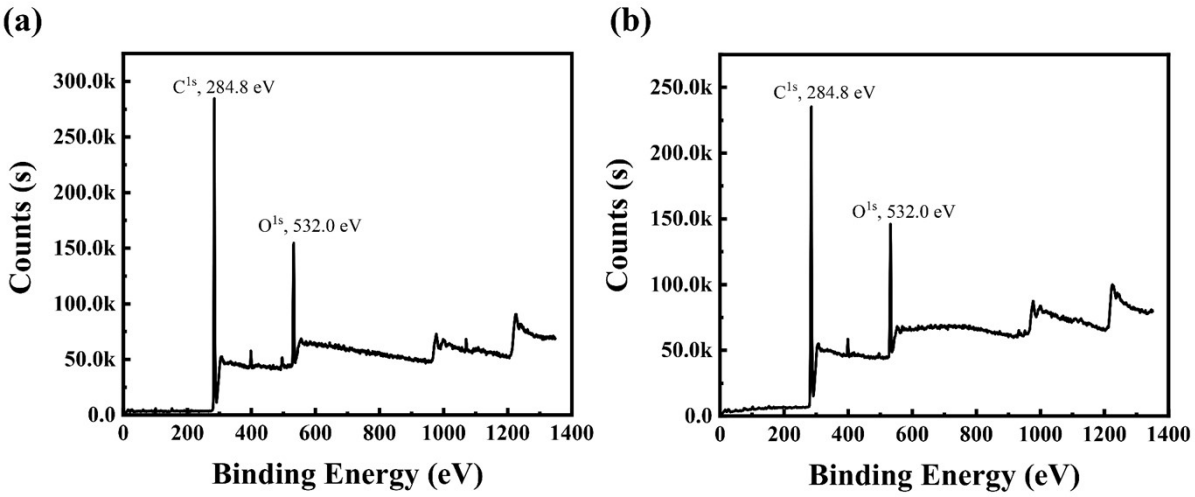

Figure S3. (a)XPS survey scan of GDY, (b) XPS survey scan of GDY/PVA membrane.

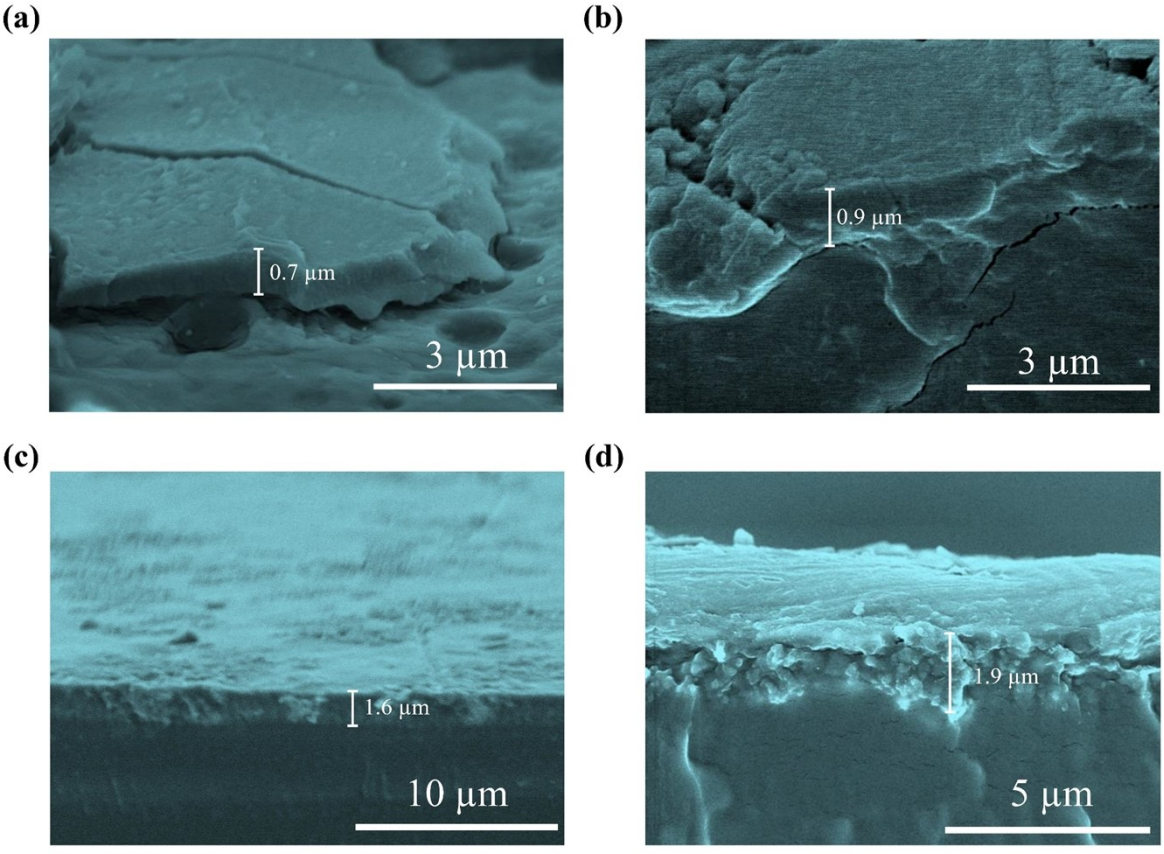

Figure S4. (a) cross-sectional SEM image of GDY/PVA-20, (b) cross-sectional SEM image of GDY/PVA-25, (c) cross-sectional SEM image of GDY/PVA-35, (d) cross-sectional SEM image of GDY/PVA-40.

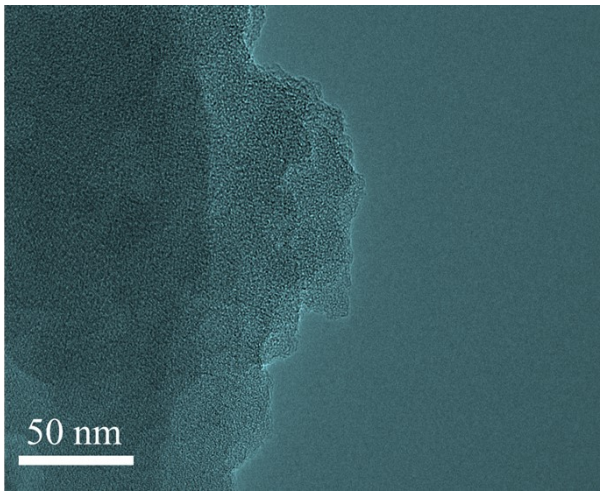

Figure S5. TEM image of GDY.

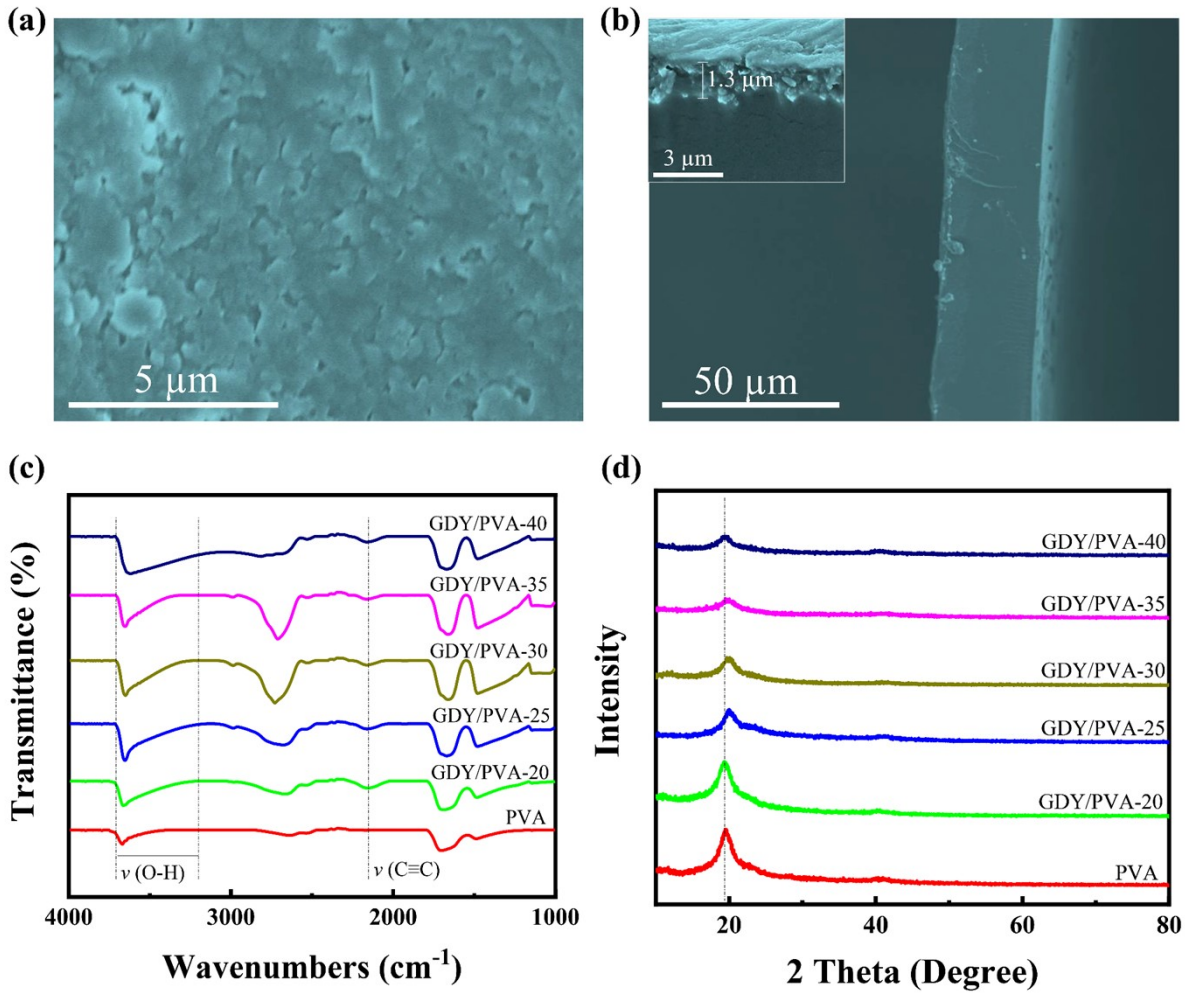

Figure S6. (a) SEM image of GDY/PVA-30 membrane, (b) cross-sectional SEM image of GDY/PVA-30 membrane at different magnifications, (c) FTIR spectra of pure PVA and hybrid membranes, (d) XRD patterns of pure PVA and hybrid membranes.

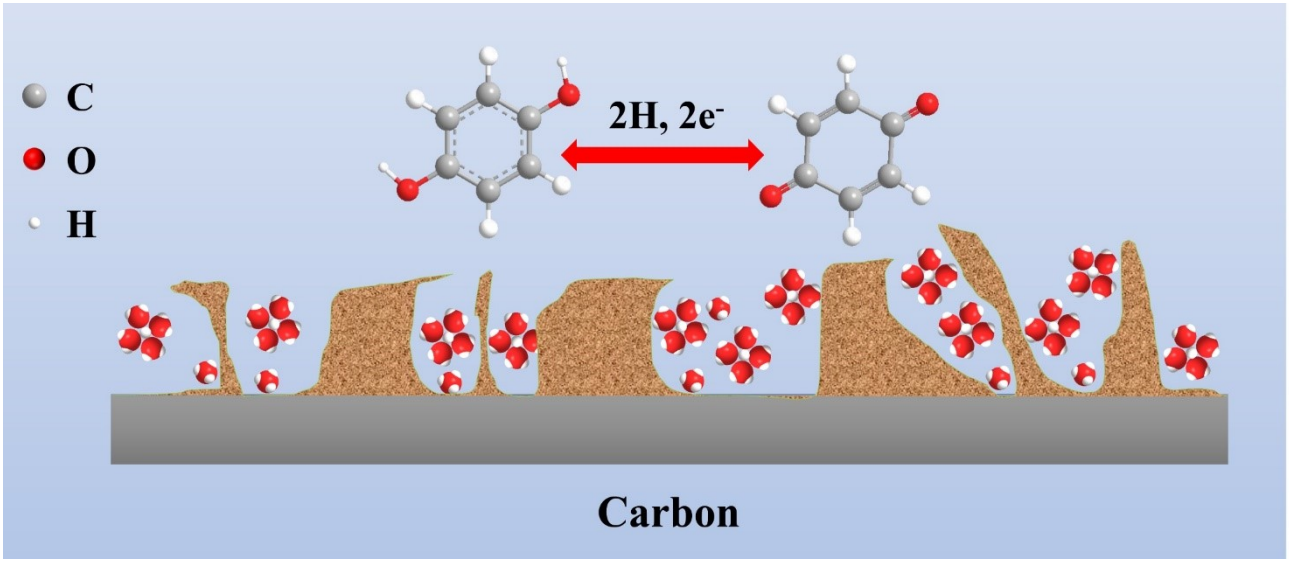

Figure S7. Redox reactions initiated by hydroquinone/ p-benzoquinone molecules.

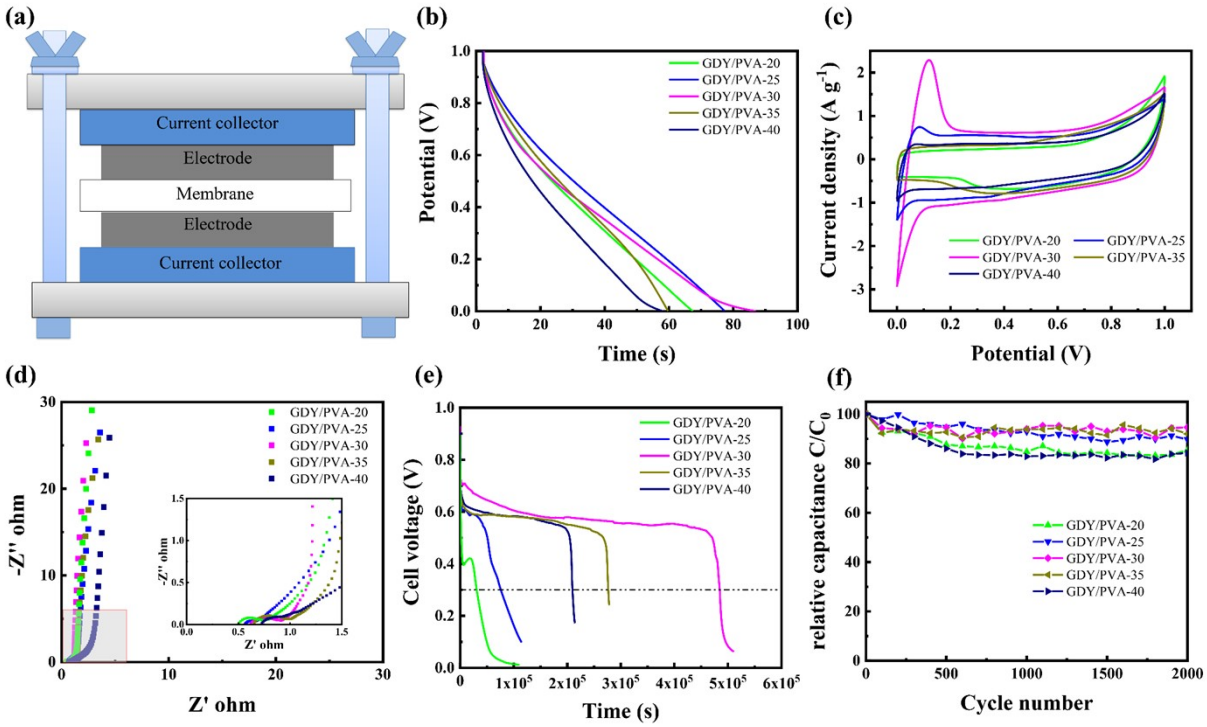

Figure S8. The electrolyte was 1 M H_2SO_4 with 0.2 M HQ added, and the membrane was composed of GDY composite films of different concentrations (a) Schematic diagram of the supercapacitor device, (b) Charge/discharge curves of supercapacitor with different membranes at current density 1 A g^{-1}, (c) CVs of supercapacitor with different membranes at scan rate of 10 mV s^{-1}, (d) EIS of supercapacitor with different membranes, (e) Self-discharge

of the supercapacitors with different membranes, (f) Cycle stability of supercapacitor at current density 1 A g^{-1}.

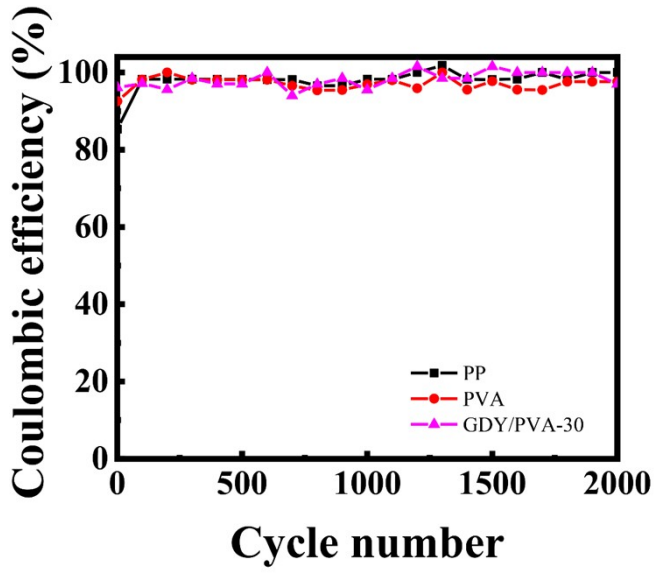

Figure S9. The coulombic efficiency of different membrane.

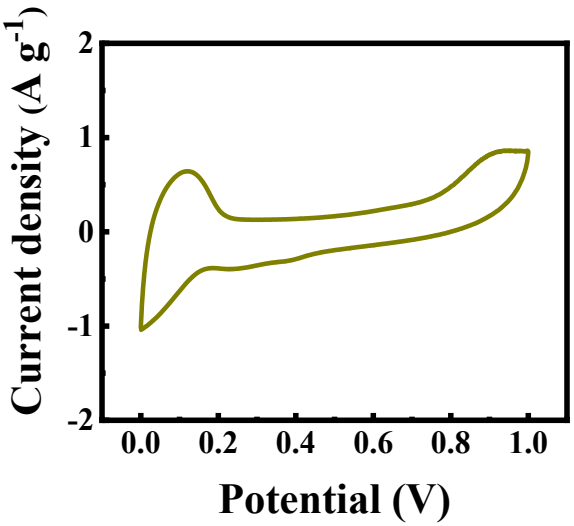

Figure S10. Cyclic voltammetry (CV) curves at a scan rate of 5 mV s^{-1} by use PVA membrane.

Table S1 Membrane thickness, Solution resistance, Charge–transfer resistance, and ionic conductivity of the membranes containing.

Sample	*Membrane thickness /μm*	*Solution resistance /R_s Ω*	*Charge–transfer resistance /R_{ct} Ω*	*ionic conductivity / 10^{-2} S cm^{-1}*
GDY/PVA-20	27.7	0.535	0.107	9.55
GDY/PVA-25	27.9	0.562	0.111	11.6
GDY/PVA-30	28.3	0.642	0.213	12.3
GDY/PVA-35	28.6	0.651	0.255	13.0
GDY/PVA-40	28.9	0.728	0.216	12.2

Table S2. Electrical properties of GDY composite membranes with different concentrations

Sample	*Specific capacitance ($F\ g^{-1}$)*	*Energy density ($Wh\ kg^{-1}$)*	*Power density ($W\ kg^{-1}$)*	*Retention capability*	*self-discharge (s, 1V-0.3V)*
PP	352.7	11.4	604.1	78.98 % after 2000 cycles	4343
PVA	294.6	9.1	590.9	81.11 % after 2000 cycles	18450
GDY/PVA-20	337.4	10.9	604.8	85.35 % after 2000 cycles	30900
GDY/PVA-25	388.8	12.6	604.4	89.74 % after 2000 cycles	75920
GDY/PVA-30	443.54	14.0	596.1	94.63 % after 2000 cycles 79.99 % after 20000 cycles	484700
GDY/PVA-35	298.7	9.7	603.7	92 % after 2000 cycles	276600
GDY/PVA-40	293.7	9.3	596.9	84.26 % after 2000 cycles	209700

Table S3. Comparison of specific capacitance and energy density with different reported values

Electrode	*Separator*	*Electrolyte*	*Specific capacitance ($F\ g^{-1}$)*	*self-discharge (s)*	*Retention capability*	*Ref.*
GHG	Nafion® 117	H_2SO_4 + HQ	C_c 75.0@ 2.1 A g^{-1}	4686 (1−0.3V)		[8]
GHG	cellulose acetate	H_2SO_4 + HQ	C_c 100.2 @1.3 A g^{-1}	1462 (1−0.3V)		[8]
GHG	cellulose acetate	$CuSO_4$+H_2SO_4	C_c 113 @ 2.1 A g^{-1}	7727 (1−0.3V)		[8]
MXene	Celgard 3501	H_2SO_4 + KI	C_c 166 @ 1A g^{-1}		100% after 5000 cycles	[9]
MWCNTs	glassy fibrous	H_2SO_4+indigo carmine	C_{sp}50@0.88mA cm^{-2}		70% after 5000 cycles	[10]
AC	polypropylene sheet	H_2SO_4+ K I	C_{sp} 912@2mA cm^{-2}	1800 (1−0.3V)	130% (5mA cm^{-2})	[2]
AC	Glass microfiber	H_2SO_4+ K I	C_{sp} 235 @1 A g^{-1}	25200 (1−0.3V)		[11]
NPS-800	Swagelok®cells	H_2SO_4 + KI	C_c 70 @0.7 A g^{-1}		86.2% after 5000 cycles	[12]
AC	Anion exchange membranes (FAS15)	SnF_2 + $VOSO_4$		21600 (1.35−1.2V)		[13]
AC	C_4mim^+−MXene Janus separator	Na_2SO_4 + KI	172 F g^{-1}@0.5A g^{-1}	86400 (1.6−1.15 V)	120% after 15 000 cycles	[14]
AC	GDYO/PVA	H2SO4 + KI	C_{sp} 325.6@1A g^{-1}	37160 (1−0.3V)	96.2% after 1000 cycles	[15]
AC	GDY/PVA	H_2SO_4 + HQ	C_{sp} 443.54@1A g^{-1}	484700 (1−0.3V)	94.63% after 2000 cycles 79.99% after 20000 cycles	This work

GHG: graphene hydrogel

MXene: $Ti_3C_2T_x$

AC: Activated carbon

References

1. G. Li, Y. Li, H. Liu, Y. Guo, Y. Li and D. Zhu, *Chem. Commun.*, 2010, **46**, 3256-3258.
2. S. T. Senthilkumar, R. K. Selvan, Y. S. Lee and J. S. Melo, *J. Mater. Chem. A.*, 2013, **1**, 1086-1095.
3. L. Q. Mai, A. Minhas-Khan, X. Tian, K. M. Hercule, Y. L. Zhao, X. Lin and X. Xu, *Nat Commun.*, 2013, **4**, 2923.
4. S. Zhang and N. Pan, *Adv. Energy Mater.*, 2015, **5**, 1401401.
5. N. Yang, S. Yu, W. Zhang, H. M. Cheng, P. Simon and X. Jiang, *Adv Mater.*, 2022, **34**, e2202380.
6. X. Chang, M. F. El-Kady, A. Huang, C. W. Lin, S. Aguilar, M. Anderson, J. Z. J. Zhu and R. B. Kaner, *Adv. Funct. Mater.*, 2021, **31**.
7. V. Sharma, U. Narayan Pan, T. Ibomcha Singh, A. Kumar Das, N. Hoon Kim and J. Hee Lee, *Chem. Eng. J.*,

2021, **415**.
8. L. Chen, H. Bai, Z. Huang and L. Li, *Energy Environ. Sci.*, 2014, **7**, 1750-1759.
9. J. Fu, L. Li, D. Lee, J. M. Yun, B. K. Ryu and K. H. Kim, *Appl. Surf. Sci.*, 2020, **504**, 144250.
10. S. Roldán, Z. González, C. Blanco, M. Granda, R. Menéndez and R. Santamaría, *Electrochim Acta.*, 2011, **56**, 3401-3405.
11. M. Meller, J. Menzel, K. Fic, D. Gastol and E. Frackowiak, *Solid State Ionics.*, 2014, **265**, 61-67.
12. K. Jayaramulu, D. P. Dubal, B. Nagar, V. Ranc, O. Tomanec, M. Petr, K. K. R. Datta, R. Zboril, P. Gomez-Romero and R. A. Fischer, *Adv Mater.*, 2018, **30**, e1705789.
13. J. Lee, B. Krüner, A. Tolosa, S. Sathyamoorthi, D. Kim, S. Choudhury, K.-H. Seo and V. Presser, *Energ Environ Sci.*, 2016, **9**, 3392-3398.
14. W. Yang, Q. Han, W. Li, M. Wu, J. Yao, M. Zhao and X. Lu, *Energy Stor. Mater.*, 2022, **52**, 29-39.
15. N. Liang, X. Wu, Y. Lv, J. Guo, X. Zhang, Y. Zhu, H. Liu and D. Jia, *J. Mater. Chem. C.*, 2022, **10**, 2821-2827.